A New Particle Swarm Optimization with Bat Algorithm Parameter-Based MPPT for Photovoltaic Systems under Partial Shading Conditions

Muhannad ALSHAREEF

Department of Communication and Electronics Engineering, College of Engineering in Al- Qunfudhah, Umm al-Qura University, Mecca, Saudi Arabia
mjshareef@uqu.edu.sa

Abstract: The characteristics of photovoltaic (PV) systems can vary, resulting in several power peaks, when partially shaded. Traditional methods, which are often used to track maximum power peak (MPP) at normal environmental conditions, are unable to detect global maximum power peak (GMPP) under partial shading condition (PSC). This paper develops a new metaheuristic optimization MPPT method to tackle this problem. The method was created by combining the best aspects of bat algorithm (BA) with particle swarm optimization (PSO). The advantages of one method remunerate for the drawbacks of the other method, in this case the proposed MPPT method has distinct advantages. In addition, the algorithm is simple and fast. PSIM simulations are undertaken under various PSC to assess the performance of the proposed method. Therefore, the results of the present method are compared through simulation with those obtained by the BA and PSO methods. The findings demonstrate how the proposed method outperforms both the BA method and the PSO method. Finally, this paper provides a comprehensive comparison of the proposed method to current soft computing methods from the literature review.

Keywords: Hybrid intelligent systems, Maximum power point tracker, Particle swarm optimization, Photovoltaic systems, Solar power generation.

1. Introduction

Recently, renewable energy sources, particularly photovoltaic (PV) energy, have sparked increased attention because of their abundance and the fact that they are eco-friendly. Lowering the energy cost provided by PV systems is a particularly active research area. There are two ways in which the cost is usually minimized. The first is to enhance the physical structure and materials of the PV cells. The second is to use power electronics circuits in conjunction with the PV array to boost the efficiency of the PV system. The latter approach is the main focus of this paper. Because P–V characteristics are nonlinear, a circuit is needed to drive the PV array at the terminal voltage matching to the maximum power. This can be achieved by employing a DC-DC converter with the integrated maximum power point technique (MPPT) to track the most maximum power points as a control approach. When the PV array contains modules exposed to uniform irradiation, the P-V characteristic contains single peak; thus, conventional MPPT approaches including perturb and observe (P&O), fractional open circuit voltage, incremental conductance and others (Kermadi et al., 2020) can be successfully applied.

Partial shading can occur if a physical item blocks irradiance from reaching the PV array. To avoid the hot-spot phenomenon, which might harm the shaded modules, every PV module must have a bypass diode connected in parallel. Nevertheless, PSC cause numerous maxima in the P–V characteristic of the PV panel. Conventional MPPT methods are ineffective and may eventually become stuck in local peaks (LPs) and fail for tracking the global peak (GP). To minimize the influence of PSC on PV arrays, a variety of evolutionary optimization strategies have recently been proposed. These have also been used to track the GP of PV panel (Seyedmahmoudian et al., 2016; Belhachat & Larbes, 2019). To detect the MPP, researchers have used the genetic algorithm (GA) (Huang et al., 2018), artificial intelligence techniques based on neural networks (ANN) (Ibenelouad et al., 2021), fuzzy logic controller (FLC) (Alshareef, 2021), for providing a complete analysis, categorization, and comparison of GMPP algorithms. The criteria for comparing the effectiveness of most GMPP techniques are simplicity in terms of hardware implementation, expense, quickness, and the precision with which the PV panels track the GMPP. The meta-heuristic approaches (MHAs) were built to tackle an optimization issue that adapts to each situation in a unique way (Savsani et al., 2016). Because P-V characteristics are rarely known in advance, MHAs are an excellent choice for solving the GMPP issue under PSC. Because of its simplicity, particle swarm optimization (PSO) is one of the most common utilized MHAs for MPPT (Zhang et al., 2020).

https://doi.org/10.24846/v31i4y202206

However, for vast search spaces, PSO suffers from a long tracking time. An enhanced PSO was used by Ishaque et al. (2012) to locate the GMPP by integrating certain parameters and then computing the duty cycle depending on the variation in power. Nevertheless, certain constants need to be determined based on the relationship between PV maximum power and duty cycle. Other MHAs for MPPT are being sought by researchers. The artificial bee colony (ABC) algorithm was used by Sundareswaran et al. (2015) to detect the GMPP under PSC, and was found to outperform PSO in terms of convergence. Regrettably, ABC will become caught in a local maximum power point (LMPP) if the number of bees is low. In (Jiang & Maskell, 2014), for application in MPPT, the ant colony optimization (ACO) approach was created. When tested in conditions with uniform and shaded patterns, the ACO algorithm performs similarly to the PSO method. Tey et al. (2018a) proposed an effective differential evolution for obtaining GMPP under PSC. With minimal control parameters, this method offers quick convergence and ease of implementation. However, there is no way to follow the past position and movement of the particle throughout the program. As a result, it is likely to become trapped at a LMPP. Inspired by the brooding habits of the Cuckoo, the Cuckoo Search (CS) was proposed by Yang & Deb (2009). In comparison to PSO, the algorithm is more effective (Kermadi et al., 2019). Yet, it has a slow rate of convergence. A new MHA known as the bat algorithm (BA), inspired by bat echolocation, was developed by Yang & Hossein Gandomi (2012). Particles were found to exhibit reduced oscillation and improved dynamic behavior when local exploitation and a global exploration process are combined. Several studies (Tey et al., 2018b; Kaced et al., 2017) have outlined the usage of BA for MPPT in order to achieve GMPP under PSC. It was verified that BA exhibits better performance than PSO and P&O (Kaced et al., 2017). Nevertheless, one disadvantage of BA is that it can easily become caught at a LMPP under certain conditions, lowering efficiency and output power of the PV system. The effectiveness of the BA algorithm for solving engineering-based optimization issues has been demonstrated in several studies (Mirjalili et al., 2014; Yılmaz & Küçüksille, 2015). Although various PSO and BA versions have been developed (Abbas et al., 2017) problems such as premature convergence and computational time delay highlight the need to create a hybrid approach to address these issues while also improving performance. In order to detect the global maximum power point, this paper proposes a hybrid method based on a combination of PSO and BA. It evaluates the proposed algorithm for a PV system under various PSC in terms of its speed and effectiveness.

The rest of the paper is structured as follows. Section 2 discusses characteristics of PV on PSC. An overview of the functioning principles of PSO and BA is provided in Section 3. Section 4 describes the proposed PSO-BA algorithm. The verification for the proposed algorithm is presented in Section 5 and the results are compared with those of other MPPT algorithms under simulation. Finally, Section 6 provides the concluding remarks.

2. PV Characteristics under PSC

Figure 1 depicts operation of PV array under uniform irradiance and PSC. Due to the series wiring of the PV modules, the current passing through them is the same. The photo current I_{sc} quickly falls to zero if a PV module is covered or shaded. Because of the reverse bias of the shaded diode, the current I_d decreases to zero; as a result, the current I leads to a drop in voltage V_c across R_p and R_s, as shown by:

$$V_c = -(R_p + R_s)I \tag{1}$$

where R_p is the shunt resistance of PV module, R_s is the series resistance of the PV module, and I is the output PV current. Because the voltage drop V_c is negative, it must be eliminated from the latest output voltage, causing a hot spot to appear in the shaded position. The emergence of the hot spot diminishes PV power while also shortening the life of PV modules. The use of bypass diodes, which may direct surplus current away from the shaded module, is an effective method for protecting the PV modules. Two PV modules linked in series are utilized to make the electrical characteristics of shading easier to analyze. Suppose one PV module is completely exposed to the sun while the other is shaded. The current that flows through the two PV modules in this example is the same due to the series connection of the modules. Because compared to an unshaded/uncoverd PV module, the shaded/covered PV module produces lower current, the bypass diode is passed by the excess current. In other words, the current in the string of PV modules must fall to the level of the shaded module (Iqbal et al., 2021).

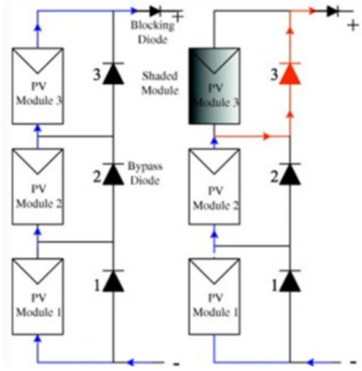

(a) (b)

Figure 1. Operation of the PV array under (a) uniform irradiance; (b) partial shading condition (Iqbal et al., 2021)

The equivalent P-V and I-V characteristics of PV array under uniform irradiance and PSC are depicted in Figure 2. As a consequence of connecting the PV modules in series, when the modules are exposed to varying levels of irradiation, several peaks appear in the output voltage, as a result of which the ultimate output power has a high number of peaks. As the number of PV modules increases along with the varying irradiation, the I-V characteristic will be more multifaceted with many peaks. As a result, tracking MPP using traditional MPPT methods is challenging.

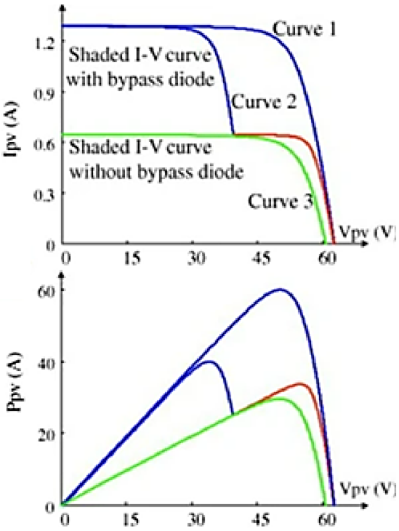

Figure 2. The P-V and I-V characteristics of PV array under uniform irradiance and PSC (Iqbal et al., 2021)

3. An Overview of the Metaheuristic Techniques

3.1 Particle Swarm Optimization

PSO is a chaotic process that can be applied to find the best solution to optimization issues. PSO relay on a mockup of a flocks of birds who, searching for the optimal location in a multi-dimensional space, increases their success by varying their motions and distances. This is the most effective method for solving optimization problems, but has the drawback of getting caught in local minima and premature convergence. In order to improve its performance, variables have been changed or new variables added to the traditional PSO formula.

PSO involves two approaches: social and cognitive (Imran et al., 2013). PSO can be represented graphically (see Figure 3). In terms of mathematics, the velocity of PSO formulas is expressed by equation (2) and the position of PSO formulas by equation (3) (Harbaoui et al., 2019).

$$v_{id}^{t+1} = wv_{id}^{t} + c_1 r_1 \left[P_{best_{id}} - x_{id}^{t} \right] + c_2 r_2 \left[G_{best_{id}} - x_{id}^{t} \right] \quad (2)$$

$$x_{id}^{t+1} = x_{id}^{t} + v_{id}^{t+1} \; i = 1, 2, ..n; d = 1, 2, ..m \quad (3)$$

where t is the index of discrete time, I denotes the index of the particle, n denotes the number of particle in a group, m represents the dimensions of the particles, d denotes the dimension taken into account, w represents the weight of inertia, c_1 and c_2 are coefficients, and r_1 and r_2 have a value between [0, 1]. P_{best} is used to store the best experience of the particle while G_{best} is used to store the best positions among all particles (Zhang & Xie, 2009). The imagined vector diagram linking PSO equations to movement of population and particle is presented in Figure 3 (Camilli, 2015).

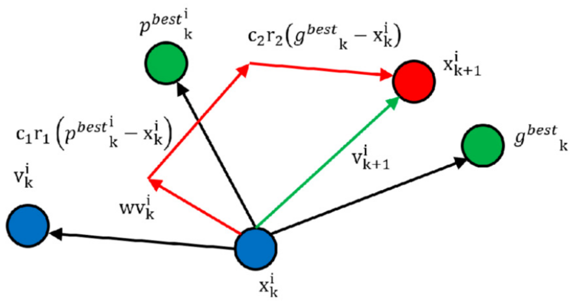

Figure 3. Process of updating particle positions (Viet et al., 2020)

3.2 Bat Algorithm

Bats do not depend on vision like other mammals. Instead, they monitor the environment using echolocation to avoid collision and capture prey. The bat first emits a sufficiently loud pulse and then gets response signals to locate its prey. The bat's pulse rate increases as the prey gets closer, while gradually decreasing their loudness. Thus, using echolocation, bats can measure target range and distinguish between obstacles and prey (Liao et al., 2020).

The bat echolocation technique inspired the BA introduced by Yang in 2010. The ideal bat procedure adheres to the below rules, which keep its biological properties:

- Using echolocation, all the bats can tell the difference between barriers and prey.
- The bats fly at speed Vi at location Xi, and alter pulse emissivity ri between [0, 1] based on the level of closeness to the prey while instantly modifying the pulse frequency.
- When the iteration number increases, the bat's loudness will gradually drop from $A0$ to $Amin$.
- The pulse frequency of the bat *i* is described as follows:

$$f_i = f_{min} + (f_{max} - f_{min})\sigma \tag{4}$$

The minimum and maximum frequencies are denoted by f_{min} *and* f_{max} respectively, and σ is a value ranging between [0, 1]. The *i th* bat's speed V_i is given by equation (5).

$$V_i^k = V_i^{k-1} + \left(X_i^{k-1} - X_{best}\right) f_i \tag{5}$$

where *k* indicates the iterations number, the present global best value is represented by X_{best}, and X_i^k is the *i th* bat position in the *k th* iteration, which is determined using equation (6) and equation (7).

$$X_i^k = X_i^{k-1} + V_i^k \ ,if\ r_k^i \le \sigma_1 \tag{6}$$

$$X_i^k = X_{best} + \beta A^{k-1}, if\ r_k^i > \sigma_1 \tag{7}$$

where r_i^k represents the *i th* bat's pulse emissivity in the *k th* iteration, $\sigma 1$ has a value between [0, 1] chosen randomly, and Ak denotes the bat's average loudness in the *k th* iteration. When $r_i^k \le \sigma_1$ appears, the bat is about to embark on a journey of global exploration.

When $r_i^k \ge \sigma_1$, bats are arriving in the local search. When the number of iterations rises, the loudness levels and pulse emissivity change. The emissivity of pulse rises and the loudness falls whenever the optimal solution remains superior to the present one. The bat is on the search for prey and moving toward it, while the loudness and pulse emissivity are adjusted. As a result, the *i* bat's loudness and pulse emissivity are specified as formulated in equation (8) (Liao et al., 2020).

$$A_i^k = \alpha A_i^{k-1} \ , r_i^k = r_i^0 \left[1 - exp\left(-\gamma k\right)\right] \tag{8}$$

where α and γ are both constant. The use of a cooling factor in the stochastic optimization algorithm (Lyden & Haque, 2016) is equivalent to the use of α in the BA. $0 < \alpha < 1$ are the value ranges. The following depicts the evaluation of loudness and pulse emissivity as the number of iterations rises:

$$A_i^k \to A_m in, r_i^k \to r_i^0, k \to \infty \tag{9}$$

Figure 4 presents the identification of the ideal position using a graphic depiction of the bat

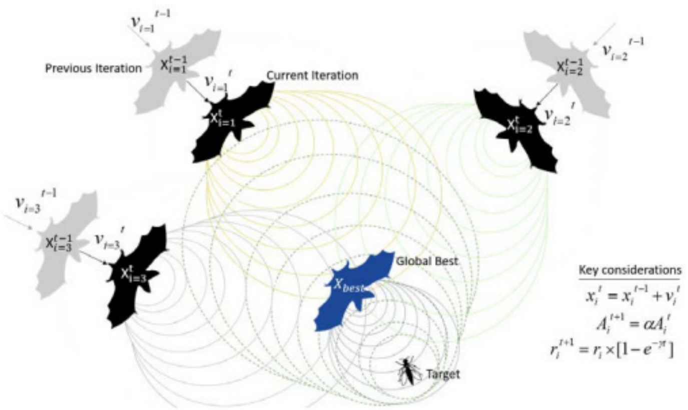

Figure 4. Mathematical representation of bat algorithm (Seyedmahmoudian et al., 2018) echolocation system as well as the process used by the bat algorithm to receive updated position and velocity vectors.

4. The Proposed Algorithm

In its standard form m PSO has a problem with becoming caught in local minima, which slows convergence and prevents the best optimal solution from being identified. BA, by contrast, is greater at exploitation but less effective at exploration in its normal form. Because of a memory deficit of the optimal solution identified so far in the optimization process, the bats frequently diverge from possible solution search space, resulting in poor exploration. This requires the establishment of procedures to prevent such problems, and the algorithms described here address these issues. The hybrid algorithm created by combining the PSO and the BA algorithms is adaptive, unique, and effective. It combines the essential elements of both methods. This study's main contribution is represented by the improvement of the performance of the conventional PSO approach, by enhancing MPPT tracking time. The proposed algorithm can successfully track the GMPP for the PV array under various PSC and exhibits better performance in comparison to the PSO and BA algorithms. In fact, for the mandated ranges provided in section 3, the proposed algorithm presents a new parameter δ which depends on cognitive social coefficient c, on the random value r of PSO, and, on the frequency component of BA derived in equation (4). The parameter can be computed mathematically as follows:

$$\delta = \left(c/r \right) f \tag{10}$$

The velocity equation of the PSO given in equation (2) is then multiplied by this factor, yielding a new velocity equation (11).

$$v_{id}^{t+1} = \delta \times [w v_{id}^{t} + c_1 r_1 [P_{best_{id}} - x_{id}^{t}] + c_2 r_2 [G_{best_{id}} - x_{id}^{t}]] \tag{11}$$

As a result, in PV applications where the hybrid PSO-BA algorithm is used, the particle position *xid* in equation (3) and equation (11) can be used to represent the PV duty cycle converter, whereas the velocity *vid* can be regarded as a duty cycle change Δdid. Equations (12) and (13) can be utilized to represent the hybrid PSO-BA approach for MPPT.

$$\Delta d_{id}^{t+1} = \delta \times \left[w\, \Delta d_{id}^{t} + c_1 r_1 \left[P_{best_{id}} - d_{id}^{t} \right] + c_2 r_2 \left[G_{best_{id}} - d_{id}^{t} \right] \right] \tag{12}$$

$$d_{id}^{t+1} = d_{id}^{t} + \Delta d_{id}^{t+1} \tag{13}$$

The best solution discovered by the particle alone is represented by (P_{best}), whereas the best solution discovered by the entire population is represented by (G_{best}) and impacts the duty cycle d_i. A large velocity value is used to update the current duty cycle d_i if it is far from these two values. P_{best}, in equation (14) is updated if the condition in equation (15) is fulfilled; otherwise, P_{best} remains at its current value. Following this, the fitness value of each particle is assessed to decide whether the value of G_{best} should be modified.

$$P_{best} = d_i^t \tag{14}$$

$$f\left(d_i^t\right) > f\left(P_{best}\right) \tag{15}$$

where f denotes the objective function that must be increased. The inertia weight w, another critical component of the PSO velocity equation, is calculated using equation (16) (Abdulkadir et al., 2014).

$$w = w_{max} - \frac{iter}{iter_{max}} \times \left(w_{max} - w_{min} \right) \tag{16}$$

where *iter* represents the iteration number.

The largest iterations number allowed is known as $iter_{max}$, w_{min} is the minimum inertia weight value, and w_{max} is the maximum inertia weight value. In comparison to existing method, the factors δ and w result in the following improvement:

- The exploitation of solutions is aided by improved particle velocity, which is achieved by influencing the BA frequency parameter.
- The ratio of PSO random variables allows for greater exploration which improves the convergence of the solution.
- They avoid getting stuck in local MPP due to a changing inertia weight parameter value via the iteration number.

The flowchart of the proposed PSO-BA algorithm is shown in Figure 5, with the following main steps addressed in detail:

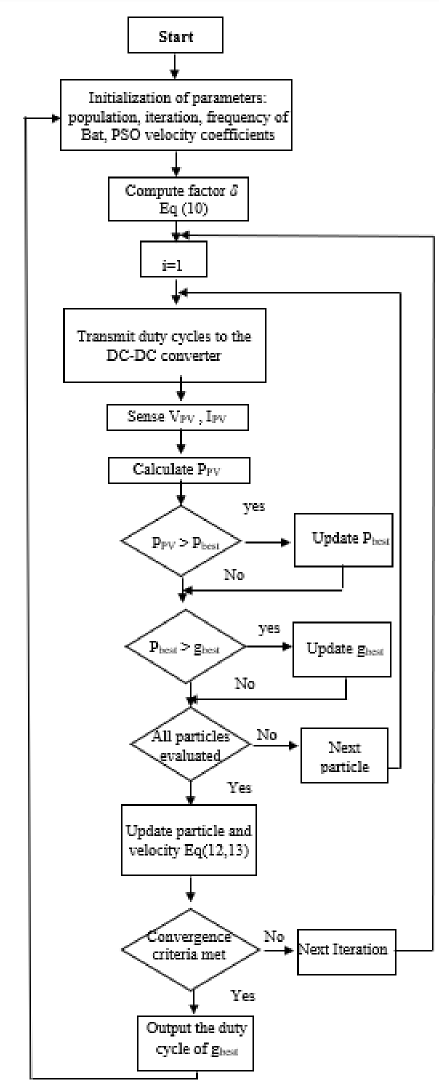

Figure 5. Flowchart of the proposed algorithm

Step 1 (Choosing a parameter): In the proposed PSO-BA algorithm, the values of requisite parameters such as population size, maximum irritation, BA frequency, PSO velocity coefficients, and inertia weight are chosen.

Step 2 (Particle initialization): The particles can be placed at specific location between d_{max} and d_{min}, which are the maximum and minimum duty cycles, correspondingly.

Step 3 (Determining the factor δ): Calculation of factor δ based on equation (10) to increase particle velocity and improve particle convergence.

Step 4 (Fitness evaluation): The PV output power is maximized using the proposed PSO-BA based MPPT technique. PV current and voltage are monitored so that PV output power may be computed as the fitness value.

Step 5 (Update the personal and global best position): The best position of the particle, reached so far is denoted as P_{best}, while the position where the best fitness is reached among all the particles visited so far is denoted as G_{best}.

Step 6 (Update the velocity and position of each particle): According to equations (12) and (13), once all of the particles have been analyzed, the position and velocity of each particle must be updated.

Step 7 (Convergence determination): The algorithm execution will be ended if the allowed iterations number has been reached, and it is presumed that the GMPP will be found.

5. Results and Discussion

5.1 Simulation of PV System Under PSCs

Like every other environmental condition, partial shading is random in nature and exhibits an unexpected pattern. As a result, there is no limit to the number of PSCs that might arise in the actual world. This study evaluates the performance of the proposed hybrid PSO-BA algorithm-based MPPT technique using three shading patterns, each representing different levels of PSC. The three conditions were selected to evaluate the proposed MPPT method. PSIM was used to run the simulation of the proposed algorithm. Figure 6 depicts the PV system model built in PSIM software. To evaluate the performance of the proposed MPPT algorithm for tracking MPP under different PSC, the proposed PV system was built, A boost converter was employed as the DC–DC converter. This boosts the voltage from the input of a PV panel.

The simulation settings for the boost converter components were as follows: $C_{in} = C_{out} = 100$ µF, L = 200 µH. The PV module utilized in the simulation had the rating listed in Table 1. The MPPT controller employed a sample period of 0.01 s. The converter had a 50-kHz switching frequency. In this study, the PV system comprised three PV modules linked in series, each with one bypass diode. As shown in Figure 7, three PSC were explored to validate the performance of the proposed method. The irradiation levels for

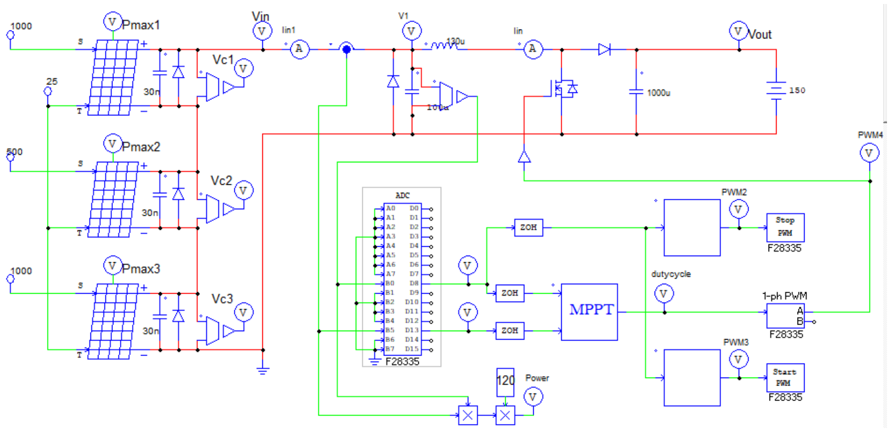

Figure 6. Model of the PV system exhibited in PSIM software

three modules are [400 W/m^2, 1000W/m^2, 800W/m^2] under the first partial shading condition. The irradiation levels for three modules are [1000W/m^2, 850W/m^2, 700W/m^2] under the second partial shading condition, while the irradiation levels for three modules are [1000W/m^2, 500W/m^2, 1000 W/m^2] under the third partial shading condition. The outcomes were evaluated with those of the traditional PSO method and BA method.

Table 1. Specification of PV module

Specification of single PV module	Values
Maximum Power (P_{mpp})	60 W
Open Circuit Voltage (V_{oc})	21.1V
Maximum Power Voltage (V_{mpp})	17.1V
Short Circuit Current (I_{SC})	3.8 A
Maximum Power Current (I_{MPP})	3.5 A
Configuration of PV module	3-Series

Case 1: Figure 7 depicts three LMPPs, with the GMPP occurring in the central of the P-V curve. The GMPP occurs at the maximum voltage of V = 36V and the maximum PV power, in this case, is 102.3 W. Figure 8 shows the simulation results for the BA method, PSO method, and proposed PSO-BA method under PSC 1. Figure 8(a) depicts the PV power waveform when the BA method is used for MPPT. As depicted, the GMPP was tracked by the BA method in 0.3 s. By contrast, the GMPP was quickly tracked using the proposed PSO-BA method in 0.16 s. (Figure 8(b)). The PSO method yielded the GMPP with a tracking time of 0.33 s (Figure 8(c)). However, it caused multiple oscillations in the present waveform, which delayed power convergence. As demonstrated in Figure 8, the proposed PSO-BA method significantly decreased the convergence time toward GMPP.

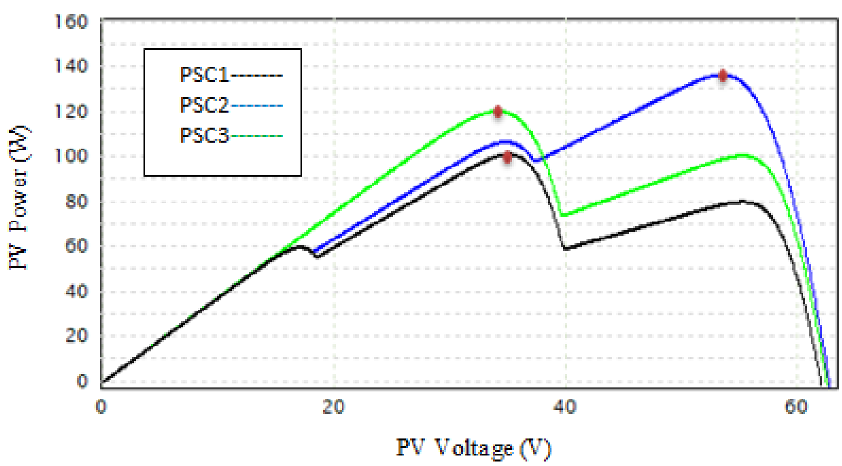

Figure 7. P-V curve under different PSC

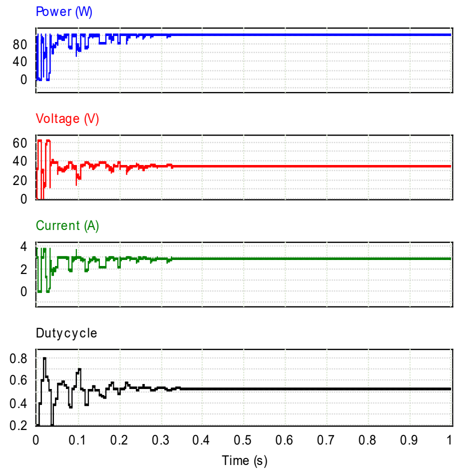

(a)

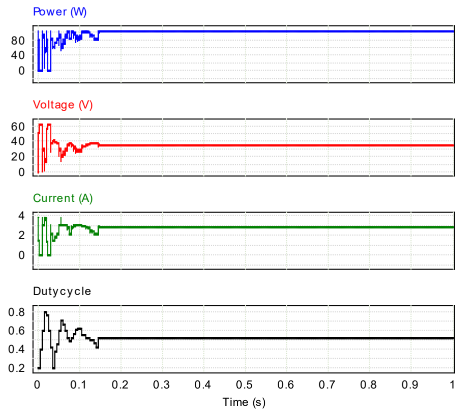

(b)

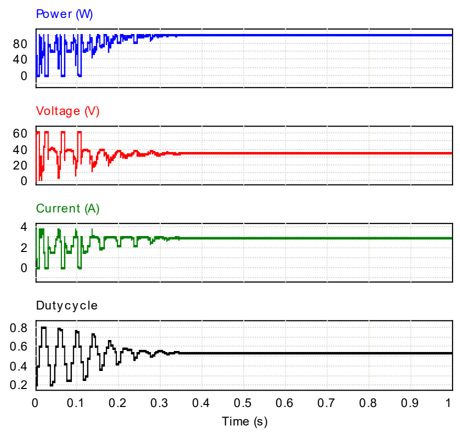

(c)

Figure 8. Comparison of voltage, power and current trajectories for PSC 1: (a) BA; (b) the proposed method; (c) PSO

Case 2: Figure 7 depicts three LMPPs, with the GMPP occurring in the rightmost of the P-V curve. The GMPP occurs at the maximum voltage of V = 54V and the maximum PV power of 138.6 W. Figure 9 shows the simulation results for the BA method, PSO method, and proposed PSO-BA method under PSC 2. Figure 9(a) shows that the BA method tracked the GMPP in 0.31 s, whereas the proposed PSO-BA method successfully obtained the GMPP in just 0.2 s with minimal oscillations, as displayed in Figure 9(b). Moreover, Figure 9(c) illustrates that the PSO method takes 0.43 s to track the GMPP. Compared with other methods, the proposed method achieves the MPP quicker.

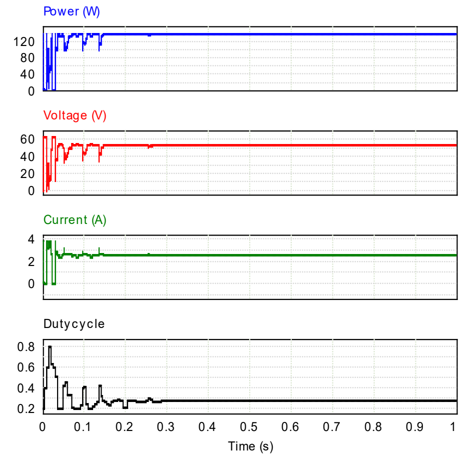

(a)

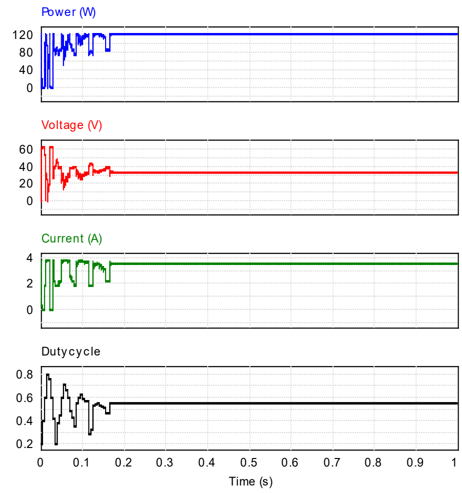

(b)

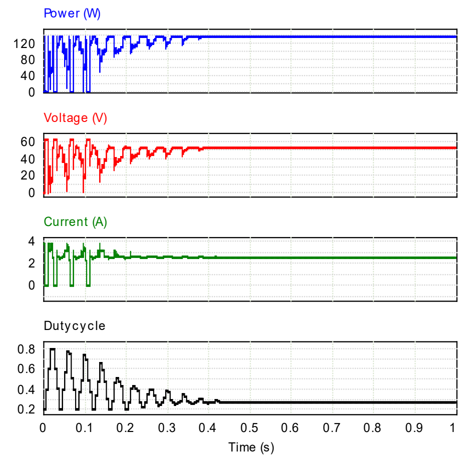

(c)

Figure 9. Comparison of voltage, power and current trajectories for PSC 2: (a) BA; (b) the proposed method; (c) PSO

Case 3: Figure 7 depicts two LMPPs, with the GMPP occurring in the leftmost of the P-V curve. The GMPP happens at the maximum voltage of V = 34V and the maximum PV power of 121.4 W. Figure 10 shows the simulation results for the BA method, PSO method, and proposed PSO-BA method under PSC 3.

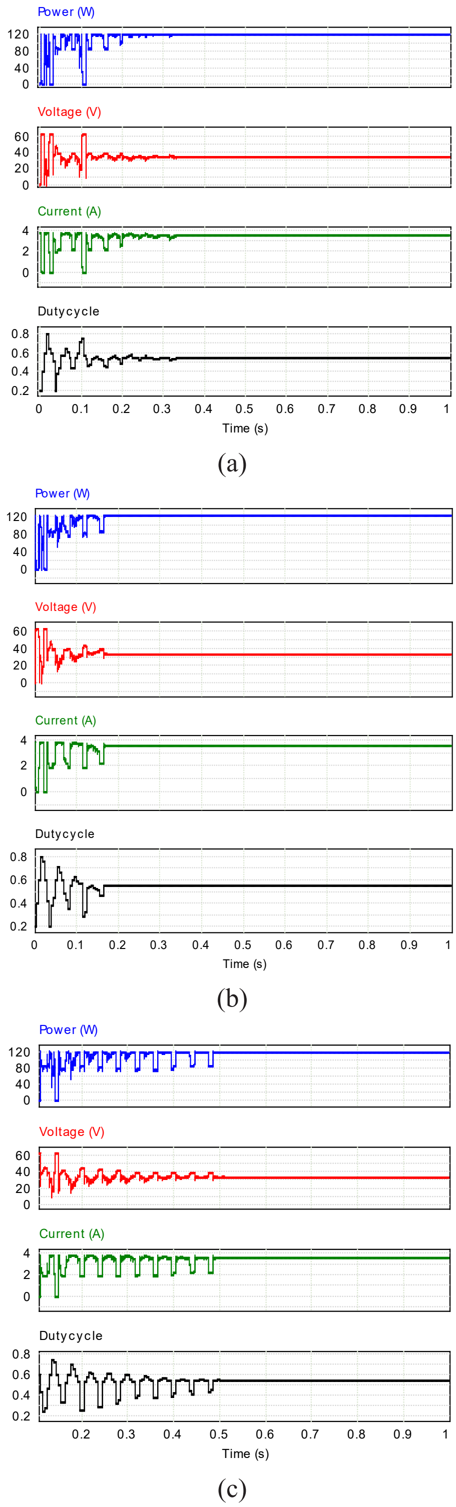

Figure 10. Comparison of voltage, power and current trajectories for PSC 3: (a) BA; (b) the proposed method; (c) PSO

Figure 10(a) indicates that the BA method was able to reach the GMPP in 0.33s but exhibited minimal power oscillations. Conversely, the proposed PSO-BA method identified the GMPP in less than 0.2 s, which is regarded as a short tracking time, as depicted in Figure 10(b). However, although the PSO method was able to track the GMPP in 0.46s, it performed poorly (Figure 10(c)). Figures 8, 9 and 10 show that the BA method performed better than PSO method in most cases. Nevertheless, compared with the proposed PSO-BA method, the BA method had a longer tracking time and larger fluctuations. For the three PSC cases, the findings indicate that, when it comes to tracking the GMPP, the proposed method performed better than the BA and PSO methods. It also displayed fewer power oscillations.

The proposed algorithm was simulated in PSIM in a one-time manner, comparable to the MATLAB-Simulink approach. As a result, after the algorithm operation was finished, the global fitness value was given. A dual conditional termination criterion was devised for the simulation tests conducted in this work to guarantee the proposed method's reliability. The halting condition arose when the fitness difference among all particles engaged was less than the predetermined threshold, or the number of iterations exceeded the predetermined iteration number that could be designed while executing the simulation results. The parameter values of the developed algorithms used in the test cases are listed in Table 2.

Table 2. The parameters and requirements of the developed algorithms used in the test cases

PSO		
Parameter	**Range**	**Value**
Inertia weight	[0-1]	W=0.6
Cognitive and social coefficient	[0-2]	C_1=1.3, C_2=1.5
BA		
Parameter	Range	Value
Frequency	[0-4]	f_{min} = 3, f_{max} = 3.25

The full findings of the tracking performances given in Table 3 indicate that the proposed PSO-BA algorithm exhibited better performance compared with other methods. It took an average of 0.18s to track the GMPP, whereas the BA and PSO took 0.31s and 0.40s, respectively, implying that more energy was obtained. Furthermore, the proposed method was the most efficient, with an average efficiency of 99.8%. All the data demonstrated that the proposed method outperformed the comparative methods in all the categories.

Table 3. Summary of the comparison findings of the proposed method with BA and PSO methods, in terms of tracking accuracy and tracking time

Methods	Cases		
	PSC1	PSC2	PSC3
Tracking Accuracy (%)			
BA	99.6	99.4	99.5
Proposed	99.8	99.9	99.7
PSO	98.8	98.4	98.7
Tracking Time (s)			
BA	0.3	0.31	0.33
Proposed	0.16	0.19	0.19
PSO	0.33	0.43	0.46

Table 4 compares the proposed PSO-BA method with existing methods, by taking into account five criteria: simplicity of parameters, tracking speed, efficiency, tracking capability and steady-state oscillation. This clearly confirms that the proposed PSO-BA method is more reliable, precise, and fast. Therefore, it represents a better choice for determining the GMPP of the PV system under different PSC.

5.2 Numerical Analysis and Discussion

Selected classical mathematical functions (Mirjalili et al., 2017) were used to assess the effectiveness of the proposed PSO-BA method. Table 5 lists the benchmark functions, where the search range represents the search space boundary, and F_{min} is the optimum.

The effectiveness of the proposed algorithm was evaluated against that of PSO algorithm and BA algorithm. The performance of the algorithms was evaluated using two indices: the mean value and the standard deviation (STD) of the best solutions that were produced in 300 separate runs.

Additionally, the convergence curves for average fitness value during the duration of iteration are provided to showcase the global search capabilities of various algorithms in the process of preventing premature convergence. Table 6 contains a summary of the quantitative findings.

Table 6 compares the mean, best, and standard deviation of fitness values for the PSO algorithm, BA algorithm and the proposed algorithm. The proposed algorithm has been shown to perform better than the other algorithms on the majority of the test benchmark functions, with the exception of the best solution and STD value for function 5.

For the selected three benchmark functions illustrated in Figure 11, all three methods exhibit convergence, with PSO having a rapid initial convergence speed. When compared to the PSO algorithm, both the BA algorithm and the proposed algorithm have a lower fitness value. While convergence speed of the PSO fell dramatically during the middle stage of the iteration, the BA algorithm and the proposed algorithm maintained

Table 4. A detailed comparison of the performance evaluation of the proposed method with several soft computing strategies

Parameters	INC (Shang et al., 2020)	PSO (Miyatake et al., 2011)	Direct (Weidong & Dunford, 2004)	Proposed method
Simplicity	Simple	Moderate	Moderate	Moderate
Efficiency	Low (under PSC)	HMh	High	Very High
GMPP tracking capability	No	yes	Moderate	High
Tracking speed	Very High	Moderate	Moderate	Very High
Steady-state oscillation	Yes	No	No	No

Table 5. Test benchmark functions

Benchmark functions	Range	f_{min}
$f_1(x) = \sum_{i=1}^{n} x_i^2$ =	[-100,100]	0
$f_2(x) = \sum_{i=1}^{n} \lvert x_i^2 \rvert + \prod_{i=1}^{n} \lvert x_i \rvert$	[-10,10]	0
$f_3(x) = \sum_{i=1}^{n} \left(\sum_{j=1}^{n} x_j\right)^2$	[-100,100]	0
$f_4(x) = max_i\{\lvert x_i \rvert, 1 \le i \le n\}$	[-100,100]	0
$f_5(x) = \sum_{i=1}^{n-1} \left(100(x_{i+1} - x_i^2)^2 + (x_i - 1)\right)^2$	[-30,30]	0
$f_6(x) = \sum_{i=1}^{n} (\lvert x_i + 0.5 \rvert)^2$	[-100,100]	0
$f_7(x) = \sum_{i=1}^{n} ix_i^4 + random\{0,1)$	[-1.28,1.28]	0
$f_8(x) = \sum_{i=1}^{n} -\left(x_i \sin\left(\sqrt{\lvert x_i \rvert}\right)\right)$	[-500,500]	-418.98 x 5
$f_9(x) = \sum_{i=1}^{n} (x_i^2 - 10\cos(2\pi x_i) + 10)$	[-5.12,5.12]	0
$f_{10}(x) = -20exp\left(-0.2\sqrt{\sum_{i=1}^{n} x_i^2}\right) - exp\left(\frac{1}{n}\sum_{i=1}^{n} cos2\pi x_i\right) + 20 + e$	[-32,32]	0
$f_{11}(x) = \frac{1}{4000}\sum_{i=1}^{n} x_i^2 - \prod_{i=1}^{n} cos\left(\frac{x_i}{\sqrt{i}}\right) + 1$	[-600,600]	0
$f_{12}(x) = \frac{\pi}{n}\{10sin(\pi y_1) + \sum_{i=1}^{n-1}(y_i - 1)^2 [1 + 10sin^2(\pi y_{i+1})] + (y_n - 1)^2\} + \sum_{i=1}^{n} u(x_i, 10, 100, 4)$	[-50,50]	0
$f_{13}(x) = 0.1\{sin^2(3\pi x_1) + \sum_{i=1}^{n}(x_i - 1)^2[1 + sin^2(3\pi x_1 + 1)] + (x_n - 1)^2[1 + sin^2(2\pi x_n)]\} + \sum_{i=1}^{n} u(x_i, 5100, 4)$	[-50,50]	0

a quick convergence throughout the process. The convergence time of the proposed method was actually quicker for the intermediate stage than the one of the BA algorithm. By the end of the iteration, both the proposed and the BA algorithm had lower fitness values in comparison with one of the PSO algorithm, and the fitness value of the proposed algorithm converged to the minimum possible value.

The findings agree with the study in subsection 5.1, which shows that combination between BA and PSO algorithms improves convergence speed and accuracy.

Table 6. Comparison of the results of three algorithms on thirteen benchmark functions

Function	Index	PSO algorithm	BAalgorithm	Proposed algorithm
f_1	Best	1.245×10^{-10}	6.734×10^{-10}	4.764×10^{-11}
	Mean	0.4642	7.3743×10^{-6}	6.384×10^{-11}
	STD	3.669	1.245×10^{-3}	2.663×10^{-11}
f_2	Best	0.0459	0.0139	1.938×10^{-7}
	Mean	2.134	1.541	3.563×10^{-7}
	STD	1.698	1.038	8.934×10^{-7}
f_3	Best	4.953	0.093	7.934×10^{-10}
	Mean	12.394	16.493	1.948×10^{-9}
	STD	19.430	20.934	1.063×10^{-9}
f_4	Best	0.376	0.00729	2.314×10^{-6}
	Mean	5.162	1.473	4.915×10^{-6}
	STD	3.193	1.593	1.228×10^{-6}
f_5	Best	0.00082	0.00561	0.85322
	Mean	162.981	211.523	130.542
	STD	228.236	335.462	374.495
f_6	Best	0.00593	0.00073	0.00035
	Mean	0.5543	0.01273	0.00387
	STD	0.0032	0.00943	0.00127
f_7	Best	0.0041	0.00169	0.00073
	Mean	0.4113	0.03295	0.00431
	STD	0.0029	0.00989	0.00365
f_8	Best	-3703.3	-3718.1	-3720.7
	Mean	-2760.5	-2766.5	-2871.3
	STD	339.832	331.183	318.452
f_9	Best	2.9934	2.98513	1.00139
	Mean	19.935	14.4648	11.1934
	STD	8.5672	7.20432	5.53224
f_{10}	Best	0.12505	1.138×10^{-5}	1.753×10^{-6}
	Mean	5.2840	2.35133	0.32412
	STD	2.0784	1.1485	0.70672
f_{11}	Best	0.06642	0.04025	2.2016×10^{-10}
	Mean	0.86342	0.33013	0.10742
	STD	0.58421	0.26291	0.08345
f_{12}	Best	0.00038	0.012456	2.8422×10^{-12}
	Mean	4.24452	2.7312	0.03732
	STD	4.37100	2.2347	0.16287
f_{13}	Best	0.00114	2.385×10^{-5}	1.239×10^{-11}
	Mean	4.19435	0.3842	0.00188
	STD	5.8294	1.4853	0.00431

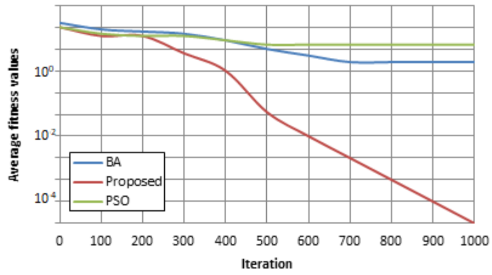

(a)

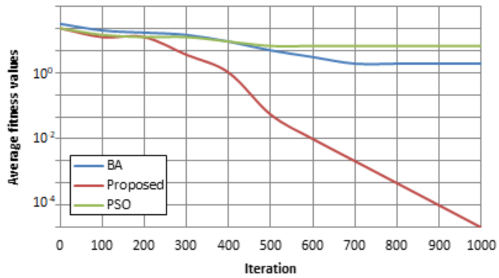

(b)

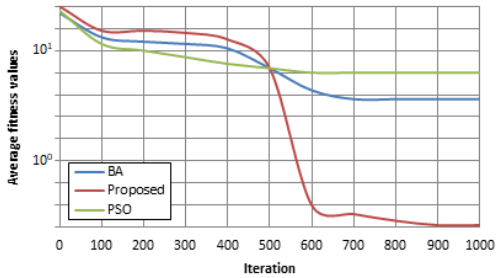

(c)

Figure 11. Convergence process for three algorithms for various benchmark functions: (a) function 1; (b) function 4; (c) function 10

6. Conclusion

This work presents an innovative metaheuristic algorithm for detecting the GMPP of a PV system under PSC. This algorithm is developed by combining the best features of PSO and BA; it presents a new factor (based on the combination between BA and PSO algorithms) which is multiplied by the equation of PSO velocity. Simulation was used to validate the proposed method under three PSCs in terms of efficiency and tracking speed of the PV system. The overall results demonstrate that the proposed method is able to detect the GMPP more effectively, and with a quicker tracking speed than the BA method and PSO method. Furthermore, a comprehensive evaluation regarding the performance of the proposed method is presented in comparison with various soft computing strategies. This indicates that the proposed PSO-BA based MPP tracking method avoids being caught at the LMPP during PSC in a more reliable and effective manner. Overall, according to the findings, the proposed method is quicker and more reliable than other methods when tested under different PSCs.

REFERENCES

Abbas, G., Gu, J., Farooq, U., Asad, M. & El-Hawary, M. (2017). Solution of an Economic Dispatch Problem Through Particle Swarm Optimization: A Detailed Survey – Part I, *IEEE Access, 5*, 15105-15141.

Abdulkadir, M., Yatim, A. & Yusuf, S. (2014). An Improved PSO-Based MPPT Control Strategy for Photovoltaic Systems, *International Journal of Photoenergy*, *2014*(7), 1-11.

Alshareef, M. (2021). An Improved MPPT Method Based on Fuzzy Logic Controller for a PV System, *Studies in Informatics and Control*, *30*(1), 89-98. DOI: 10.24846/v30i1y202108

Belhachat, F. & Larbes, C. (2019). Comprehensive review on global maximum power point tracking techniques for PV systems subjected to partial shading conditions, *Solar Energy*, *183*, 476-500.

Camilli, L. (2015). *The Evolution of Swarm Intelligence and Applications for Econometric Modelling*, Report number: 1215. Department of Computer Science, San Francisco State University, San Francisco, CA, USA.

Harbaoui, I., Ben-Alaia, E. Borne, P. & Hanen Bouchriha, H. (2019). Optimization of m-MDPDPTW Using the Continuous and Discrete PSO, *Studies in Informatics and Control, 28*(3), 289-298. DOI: 10.24846/v28i3y201905

Huang, Y., Chen, X. & Ye, C. (2018). A Hybrid Maximum Power Point Tracking Approach for Photovoltaic Systems under Partial Shading Conditions Using a Modified Genetic Algorithm and the Firefly Algorithm, *International Journal of Photoenergy*, *2018*, 1-13.

Ibenelouad, A., EL-Kari, A., Ayad, H. & Mjahed, M. (2021). Multilayer Artificial Approach for Estimating Optimal Solar PV System Power Using the MPPT Technique, *Studies in Informatics and Control*, *30*(4), 109-120. DOI: 10.24846/v30i4y202110

Imran, M., Hashim, R. & Khalid, N. E. A. (2013). An Overview of Particle Swarm Optimization Variants, *Procedia Engineering, 53*, 491-496.

Iqbal, B., Nasir, A. & Murtaza, A. F. (2021). Stochastic maximum power point tracking of photovoltaic energy system under partial shading conditions, *Protection and Control of Modern Power Systems, 6*(1). DOI: 10.1186/s41601-021-00208-9

Ishaque, K., Salam, Z., Amjad, M. & Mekhilef, S. (2012). An Improved Particle Swarm Optimization (PSO) – Based MPPT for PV With Reduced Steady-State Oscillation, *IEEE Transactions on Power Electronics, 27*(8), 3627-3638.

Jiang, L. & Maskell, D. (2014). A uniform implementation scheme for evolutionary optimization algorithms and the experimental implementation of an ACO based MPPT for PV systems under partial shading. In *2014 IEEE Symposium on Computational Intelligence Applications in Smart Grid (CIASG*), (pp. 1-8).

Kaced, K., Larbes, C., Ramzan, N. Bounabi, M. & Dahmane, Z. (2017). Bat algorithm based maximum power point tracking for photovoltaic system under partial shading conditions, *Solar Energy*, *158*, 490-503.

Kermadi, M., Salam, Z., Ahmed, J. & Berkouk, E. (2019). An Effective Hybrid Maximum Power Point Tracker of Photovoltaic Arrays for Complex Partial Shading Conditions, *IEEE Transactions on Industrial Electronics*, *66*(9), 6990-7000.

Kermadi, M., Salam, Z., Eltamaly, A., Ahmed, J., Mekhilef, S. & Larbes, C. (2020). Recent developments of MPPT techniques for PV systems under partial shading conditions: a critical review and performance evaluation, *IET Renewable Power Generation*, *14*(4), 3401-3417.

Liao, C., Subroto, R., Millah, I., Lian, K. & Huang W. (2020). An Improved Bat Algorithm for More Efficient and Faster Maximum Power Point Tracking for a Photovoltaic System Under Partial Shading Conditions, *IEEE Access, 8*, 96378-96390.

Lyden, S. & Haque, M. E. (2016). A simulated annealing global maximum power point tracking approach for PV modules under partial shading conditions, *IEEE Transactions on Power Electronics, 31*(6), 4171-4181.

Mirjalili, S. M. et al. (2017). Salp Swarm Algorithm: A bio-inspired optimizer for engineering design problems, *Advances in Engineering Software*, *114*, 163–191.

Mirjalili, S., Mirjalili, S. M. & Yang, X. (2014). Binary bat algorithm, *Neural Computing and Applications*, *25*(3-4), 663-681.

Miyatake, S., Veerachary, M., Toriumi, F., Fujii, N. & Ko, H. (2011). Maximum power point tracking of multiple photovoltaic arrays: A PSO approach, *IEEE Transactions on Aerospace and Electronic Systems*, *47*(1), 367–380.

Savsani, V., Jhala, R. L. & Savsani, V. J. (2016). Comparative Study of Different Metaheuristics for the Trajectory Planning of a Robotic Arm, *IEEE Systems Journal*, *10*(2), 697-708.

Seyedmahmoudian, M., Horan, B., Soon, T. K., Rahmani, R., Muang Than, Oo, A., Mekhilef, S. & Stojcevski, A. (2016). State of the art artificial intelligence-based MPPT techniques for mitigating partial shading effects on PV systems – A review, *Renewable & Sustainable Energy Reviews, 64*, 435-455.

Seyedmahmoudian, M., Kok Soon, T., Jamei, E., Thirunavukkarasu, G., Horan, B., Mekhilef, S. & Stojcevski, A. (2018). Maximum Power Point Tracking for Photovoltaic Systems under Partial Shading Conditions Using Bat Algorithm, *Sustainability*, *10*(5), article ID: 1347.

Shang, L., Guo, H. & Zhu, W. (2020). An improved MPPT control strategy based on incremental conductance algorithm, *Protection and Control of Modern Power Systems*, *5*(1), article number: 14. DOI: 10.1186/s41601-020-00161-z

Sundareswaran, K., Sankar, P., Nayak, P., Simon, S. & Palani, S. (2015). Enhanced Energy Output from a PV System Under Partial Shaded Conditions Through Artificial Bee Colony, *IEEE Transactions on Sustainable Energy*, 6(1), 198-209.

Tey, K. S., Mekhilef, S. & Seyedmahmoudian, M. (2018a). Implementation of BAT Algorithm as Maximum Power Point Tracking Technique for Photovoltaic System Under Partial Shading Conditions. In *2018 IEEE Energy Conversion Congress and Exposition (ECCE)*, (pp. 2531-2535).

Tey, K. S, Mekhilef, S., Seyedmahmoudian, M., Horan, B., Oo, A. T. & Stojcevski. A. (2018b). Improved Differential Evolution-Based MPPT Algorithm Using SEPIC for PV Systems Under Partial Shading Conditions and Load Variation, *IEEE Transactions on Industrial Informatics*, *14*(10), 4322-4333.

Viet, D. T., Phuong, V. V., Duong, M. Q. & Tran, Q. T. (2020). Models for short-term wind power forecasting based on improved artificial neural network using particle swarm optimization and genetic algorithms, *Energies*, *13*(11), article ID: 2873. DOI: 10.3390/en13112873

Weidong, X. & Dunford, W. G. (2004). A modified adaptive hill climbing MPPT method for photovoltaic power systems. In *Proceedings of the 2004 IEEE 35th Annual Power Electronics Specialists Conference,* Aachen, Germany (pp. 1957-1963).

Yang, X. S. (2010). A new metaheuristic Bat inspired algorithm. In González, J. R., Pelta, D. A., Cruz, C., Terrazas, G. & Krasnogor, N. (eds)., *Nature Inspired Cooperative Strategies for Optimization (NICSO 2010)*, *Studies in Computational Intelligence*, *vol 284*, 65-74. Springer, Berlin, Heidelberg. DOI: 10.1007/978-3-642-12538-6_6

Yang, X. S. & Deb, S. (2009). Cuckoo Search via Lévy flights. In *2009 World Congress on Nature & Biologically Inspired Computing (NaBIC),* (pp. 210-214). DOI: 10.1109/NABIC.2009.5393690

Yang, X. & Hossein Gandomi, A. (2012). Bat algorithm: a novel approach for global engineering optimization, *Engineering Computations*, *29*(5), 464-483.

Yılmaz, S. & Küçüksille, E. U. (2015). A new modification approach on bat algorithm for solving optimization problems, *Applied Soft Computing*, *28*, 259-275.

Zhang, J., Cui, M. & He, Y. (2020). Robustness and adaptability analysis for equivalent model of doubly fed induction generator wind farm using measured data, *Applied Energy*, *261*, article ID: 114362.

Zhang, J. & Xie, L. (2009). Particle swarm optimization algorithm for constrained problems, *Asia-Pacific Journal of Chemical Engineering, 4*(4) 437-442.